On the Relation between Bonding and the Spin−Orbit Interaction in BNe: the $C^2\Delta$ and $1^4\Pi$ States

Karl Sohlberg*,† and David R. Yarkony*,‡

Department of Chemistry, The Johns Hopkins University, Baltimore, Maryland 21218

Received: July 10, 1997[⊗]

The $C^2\Delta$ state of BAr does not fluoresce whereas the $C^2\Delta$ state of BNe does [Yang, X.; Hwang, E.; Dagdigian, P. J. *J. Chem. Phys.* **1996**, *104*, 599]. Two explanations are possible: in BNe, the spin−orbit interaction is too weak to quench the fluorescence or the location of the $C^2\Delta-1^4\Pi$ intersection is unfavorable. In this work computational techniques are used to study the spin−orbit induced predissociation of BNe($C^2\Delta$, v) and its relation to the origin of bonding in $C^2\Delta$.

1. Introduction

Once thought to be inert, the rare gases (group VIII elements) are now known to have a rich and fascinating chemistry.[1] The existence of various metal/rare-gas ionic solids has been predicted based on thermodynamic principles.[2] In fact, gas phase metal/rare-gas diatomic molecules are quite easily prepared in a free jet expansion and have been the subject of extensive spectroscopic studies.[3] Such species have received attention in part because of the potential application of boron compounds in novel high energy density propellants.[4,5] The scope of the reactivity of the rare gases is greatly enhanced by electronic excitation and electronically excited states[6−8] of metal/rare-gas molecules have been found to have surprisingly strong bonding. For example, $D_e \approx 3700$ cm^{-1} has been reported in BAr $C^2\Delta$ by Yang et al.[8] This state could not be probed directly by laser induced fluorescence (LIF), however, but only indirectly with laser depletion techniques. In a theoretical work complementary to Yang et al.,[8] we demonstrated that, as a consequence of the heavy atom effect (HAE),[9] the spin−orbit induced predissociation of BAr $C^2\Delta$ by BAr $1^4\Pi$ is sufficiently rapid to suppress any observable fluorescence signal.[10] Detailed analysis of the spin−orbit interaction revealed a type of dative bonding as the origin of the large D_e for BAr $C^2\Delta$.

In contrast to BAr $C^2\Delta$, the isovalent BNe $C^2\Delta$ state, which is much less strongly bound than BAr $C^2\Delta$,[11] has been probed successfully with LIF and does not predissociate appreciably.[12] Two explanations for this situation are possible, weak spin−orbit coupling owing a reduced HAE attributable the replacement of Ar by Ne, or an unfavorable location of the crossing, or closest approach, point of the $1^4\Pi$ and $C^2\Delta$ potential energy curves. Dagdigian and co-workers[11] have inferred from spectroscopic data that in BNe the $1^4\Pi-C^2\Delta$ crossing is high on the repulsive inner limb.[11] The size of the spin−orbit coupling and role of the HAE could not be determined in these experiments, however.

The purpose of this paper is therefore 2-fold: (i) to establish the mechanism of the (slow) predissociation of $C^2\Delta$ considering both the $1^4\Pi-C^2\Delta$ crossing and the geometry dependent $C^2\Delta-1^4\Pi$ spin−orbit coupling, and (ii) to compare the bonding in BNe $C^2\Delta$ with that in BAr $C^2\Delta$.

2. Theoretical Methods

The present calculations employed multireference configuration−interaction (MRCI) wave functions to determine the BNe $C^2\Delta$ and $1^4\Pi$ Born−Oppenheimer potential energy curves (PECs). For purposes of comparison, the methods used here are the same as those used in our earlier calculations on BAr.[10,13] Details can be found therein; however, an outline will be provided here.

State-averaged multiconfiguration self-consistent-field[14,15] (SA-MCSCF) molecular orbitals were generated for use in a second-order configuration−interaction (SOCI) calculation. As with the earlier BAr calculations, included in the state averaging were the $X^2\Pi$, $1^4\Pi$, and $C^2\Delta$ states and the weighting vector was taken as (1,1,2). The boron atomic orbital basis set used was derived from the correlation-consistent augmented valence-triple-ζ basis of Dunning.[16] The contracted [5s/4p/3d/2f] version of the original B(11s/6p/3d/2f) basis was truncated by removing the most diffuse f-function and augmented with an extra d-function, (exponent 0.0185). This is the TZ1F [5s/4p/4d/1f] basis set of ref 13. The polarized valence-quadruple-ζ basis of Dunning,[16] (Ne(12s/6p/3d/2f/1g) contracted to [5s/4p/3d/2f/1 g] with the g-function truncated) was used on neon. Two different active spaces were used in the CI calculations: (i) AS1 consisted of B 2s, $2p_x$, $2p_y$, $2p_z$, and Ne $2p_x$, $2p_y$, $2p_z$. (ii) AS2 consisted of B 2s, $2p_x$, $2p_y$, $2p_z$, and Ne $2p_x$, $2p_y$. In the MCSCF, only B 2s, $2p_x$, $2p_y$, and $2p_z$ were active. Here we have labeled the molecular orbitals by their dominant atomic orbital components, (i.e., Ne 1s, 2s, $2p_x$, $2p_y$, $2p_z$, etc. and B 1s, 2s, $2p_x$, $2p_y$, $2p_z$, etc.) which is an excellent approximation because BNe, to an even greater degree than BAr, is weakly interacting. This labeling will be employed throughout. Note that AS2 does not include Ne $2p_z$, (in MO notation, 4σ) correlation. With these active spaces the SOCI spaces are of dimension, AS1 6.9×10^6 configuration state functions (CSFs) and AS2 1.4×10^6 CSFs. These levels of treatment will be denoted ASi−SOCI, $i = 1, 2$. When the multireference version of the Davidson correction[17−19] is included the level of treatment is denoted ASi−SOCI/DC.

The AS1−SOCI (and for comparison AS1−first-order CI, AS1−FOCI) wave functions were used to compute the $1^4\Pi-C^2\Delta$ spin−orbit interaction

$$H^{so}(1^4\Pi,C^2\Delta) = i\,\langle \Psi_{1^4\Pi(3/2)}\,|H^{so}|\,\Psi_{C^2\Delta(1/2)}\rangle \qquad (1)$$

including both the one-electron spin−orbit and two-electron spin-same-orbit and spin-other-orbit terms in the Breit−Pauli Hamiltonian H^{so}.[20] M_S is given parenthetically.

† Present address: 4500N MS6197, Oak Ridge National Laboratory, Oak Ridge, TN 37831.

‡ Supported in part by AFOSR Grant F496209610017.

⊗ Abstract published in *Advance ACS Abstracts,* November 15, 1997.

S1089-5639(97)02242-1 CCC: $14.00

Finally, using $H^{so}(1^4\Pi,C^2\Delta)$ the predissociation rates were computed for BNe $C^2\Delta$ with the perturbative Fermi golden rule (FGR) approximation.[21,22] Comparison of spin−orbit induced predissociation rates computed with the FGR approximation to those from numerically exact resonance calculations[23,24] for the BAr system showed excellent agreement.[10] Since the spin−orbit interaction of concern here is even weaker than that in BAr, it is reasonable to expect that the FGR approximation will be excellent in the present case as well.

3. Results and Discussion

3.1. Potential Energy Curves. In BNe, the $1^4\Pi$ state arises from the interaction of B ($2s2p^2$ ^4P) with ground-state Ne(^1S) and the $C^2\Delta$ state arises from the interaction of B ($2s2p^2$ ^2D) with Ne(^1S). Asymptotically, the states are separated by 18980 cm^{-1}, the separation of the corresponding ^4P and ^2D boron atomic terms.[25] A semiquantitative picture of the low-lying electronic states of BNe is given in ref 11. There is a higher energy ^2D term arising from the nominally $2s^23d^1$ Rydberg configuration of atomic boron which has important implications for describing the $C^2\Delta$ state. This is discussed at length in ref 13, where a detailed discussion of the low-lying electronic states of the isovalent BAr is also given.

PECs for BNe $C^2\Delta$ computed at the AS1−SOCI, AS1−SOCI/DC, and AS2−SOCI levels are shown in Figure 1a. Note in particular that the AS2−SOCI level, which does not include correlation of the 4σ (nominally Ne $2p_z$) orbital, greatly underestimates the bond strength as compared to AS1−SOCI and experimental values.[12] The residual binding, on the order of 50 cm^{-1}, is similar to that seen in isovalent BAr when the corresponding orbital, the 6σ orbital, is uncorrelated. This provides important insight into the nature of the bonding in BNe $C^2\Delta$, an issue to be addressed below. Spectroscopic constants for BNe $C^2\Delta$, computed with methods which *do* include correlation of the 4σ orbital, are given in Table 1 where a comparison is made with experimentally derived values. Also given are the separations of the vibrational levels of the $C^2\Delta$ state. The agreement with experiment is seen to be very good to excellent, confirming the validity of the computational methods employed for the BNe system.

Figure 1b shows both the BNe $C^2\Delta$ and $1^4\Pi$ PECs on the same horizontal scale as Figure 1a, but with an expanded vertical energy scale to show the location of the $C^2\Delta-1^4\Pi$ crossing. This crossing is high on the inner limb, 4383[3463] cm^{-1} above the dissociation asymptote of the $C^2\Delta$ state, at the AS1−SOCI-[AS1−SOCI/DC] level. As evinced in Table 1 there is the excellent agreement between the spectroscopically inferred position of the $C^2\Delta-1^4\Pi$ crossing and the computed value.

Although the results at both the AS1−SOCI and AS1−SOCI/DC levels are very reasonable, the AS1−SOCI/DC treatment gives some improvement in the *shape* of the $C^2\Delta$ PEC over that achieved with the AS1−SOCI method, (as evidenced by the improved agreement of ω_e, $\omega_e x_e$, and the vibrational ladder spacings, with the spectroscopically derived values of these parameters) but at the expense of a somewhat less accurate value D_e.

One noteworthy point is that the equilibrium separation in BNe $C^2\Delta$ is considerably larger than that in isovalent BAr. Since the atomic radius of Ar is larger than that of Ne, the smaller value of R_e in BAr must result from a greater degree of true "chemical" bonding where electrons are being shared. Indeed the bonding in BAr $C^2\Delta$ has been shown to result from dative bonding where the Ar furnishes a pair of electrons and B supplies the empty valence orbitals.[13] We will return to this issue once again below.

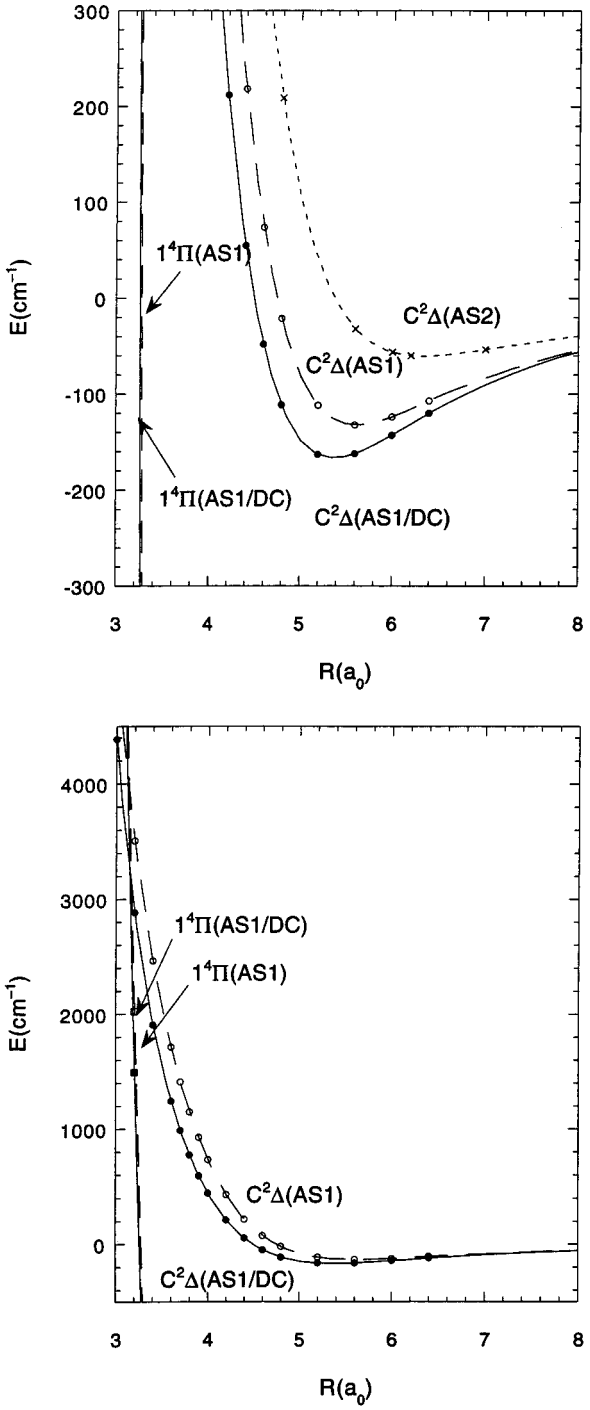

Figure 1. Upper part shows PECs for BNe $C^2\Delta$ computed at three levels of theory. solid circles, AS1−SOCI/DC; open circles, AS1−SOCI; crosses, AS2−SOCI. AS1−SOCI/DC and AS1−SOCI are shown for the $1^4\Pi$ state with unmarked solid and dashed curves, respectively. Lower part shows $C^2\Delta$ PECs as well as $1^4\Pi$ PECs on the same horizontal scale as upper part, but with an extended vertical energy scale to show the location of the $C^2\Delta-1^4\Pi$ crossing. Point markers are as in upper part for $C^2\Delta$. For $1^4\Pi$, solid squares, AS1−SOCI/DC; open squares, AS1−SOCI. The curves connecting the points are spline fits used for visual clarity.

3.2. Spin−Orbit Interaction. Having established the reliability of the PECs, we next address the spin−orbit coupling between BNe $1^4\Pi$ and $C^2\Delta$. Figure 2 shows the spin−orbit coupling matrix element $H^{so}(1^4\Pi,C^2\Delta)(R)$ for $\{3.0 \le R \le 8.0$ $a_0\}$. When interpreted within a single CSF picture, the spin−orbit coupling surrenders a second important clue about the nature of the bonding in BNe $C^2\Delta$.

TABLE 1: Geometric and Spectroscopic Parameters

parameter	exptl	AS1−SOCI/DC[b]	AS1−SOCI[b]
D_e	138.3[c]	170.5	138.1
R_e	5.42[d]	5.40	5.68
R_x	3.17[e]	3.11	3.08
ω_e	59.5[f]	60.3	53.0
$\omega_e x_e$	6.4[f]	8.1	8.6
$\nu = 0$	46.8[f]	45.6	37.9
$\nu = 1$	33.6[f]	33.6	26.7
$\nu = 2$	20.8[f]	24.4	19.4

[a] Geometric and spectroscopic parameters as well as vibrational ladder spacings ($E_{\nu+1} - E_\nu$) for BNe $C^2\Delta$. Units are cm^{-1} and a_0. [b] Present work. [c] Derived from the ω_e and $\omega_e x_e$ values in ref 12 as per ref 29. [d] From ref 11. [e] Interpolated from Figure 5 in ref 11. [f] From ref 12.

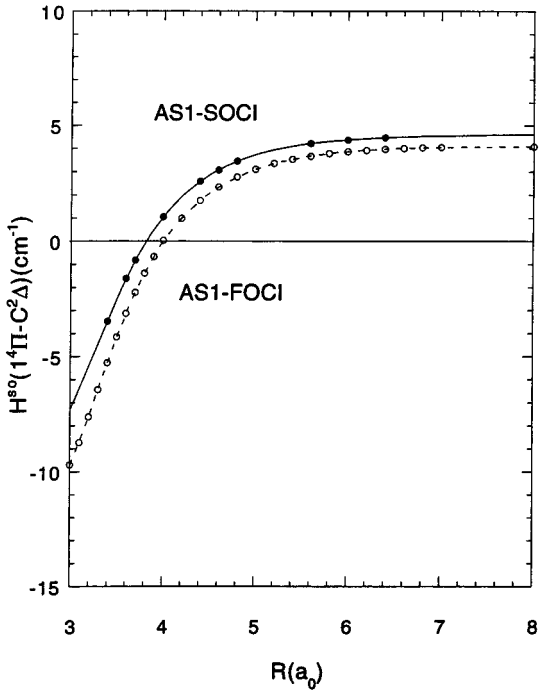

Figure 2. Spin-orbit coupling $H^{so}(1^4\Pi,C^2\Delta)(R)$ as a function of R. Open circles are based on FOCI wave functions; solid circles are based on SOCI wave functions. Adjacent points are joined with line segments.

The following analysis closely parallels that of the $C^2\Delta-1^4\Pi$ spin−orbit coupling in BAr.[13]

In the single CSF model and using a one-electron approximation to the spin−orbit operator,[20]

$$H^{so}(1^4\Pi,C^2\Delta) \approx \langle 6\sigma|h_x^{so}|\ 2\pi_y\rangle \qquad (2)$$

The 6σ and $2\pi_y$ orbitals are described qualitatively by

$$6\sigma \approx s_1(R)\mathrm{B}(2p_z) + s_2(R)\mathrm{Ne}(2p_z)$$

$$2\pi_y \approx r_1(R)\mathrm{B}(2p_y) - r_2(R)\mathrm{Ne}(2p_y) \qquad (3)$$

A picture of the qualitative behavior of $s_1(R)$ and $s_2(R)$ is afforded by Figure 3 where the relative contributions of the dominant atomic basis functions to the 6σ orbital are shown as a function of R. The 2p basis functions have a nodal structure correct for the given principle quantum number, but the more diffuse basis functions (denoted p,[3] p[4], etc.) are nodeless. At large values of R, $s_1(R) \approx 1$ and $s_2(R) \approx 0$. As R decreases, neon-centered basis functions make an ever greater (antibonding) contribution to the molecular orbital so that s_2 increases. A similar analysis for the $2\pi_y$ orbital is depicted in Figure 4 where again the molecular orbital is seen to become increasingly

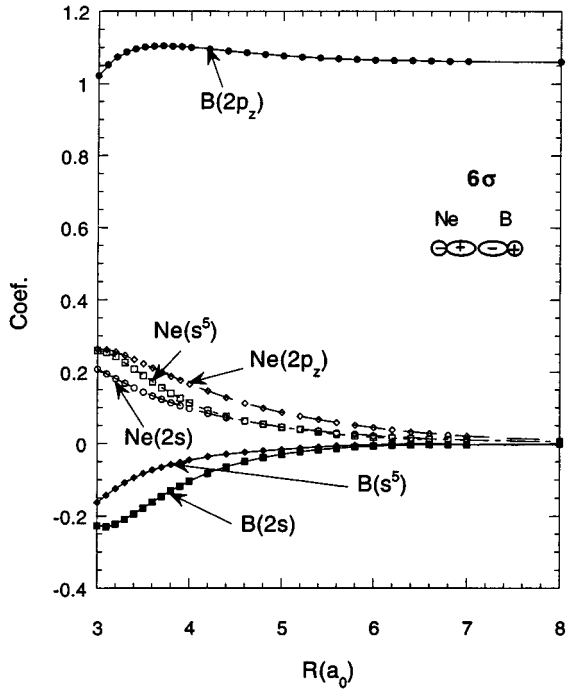

Figure 3. Dominant atom-centered basis function contributions to the 6σ (nominally B $2p_z$) orbital. Point markers: Solid circles denote the contribution from the B $2p_z$ orbital; open diamonds, Ne $2p_z$; open squares, Ne s^5; open circles, Ne 2s; solid diamonds, B s^5; solid squares, B 2s. The interaction is antibonding. Adjacent points are joined with line segments.

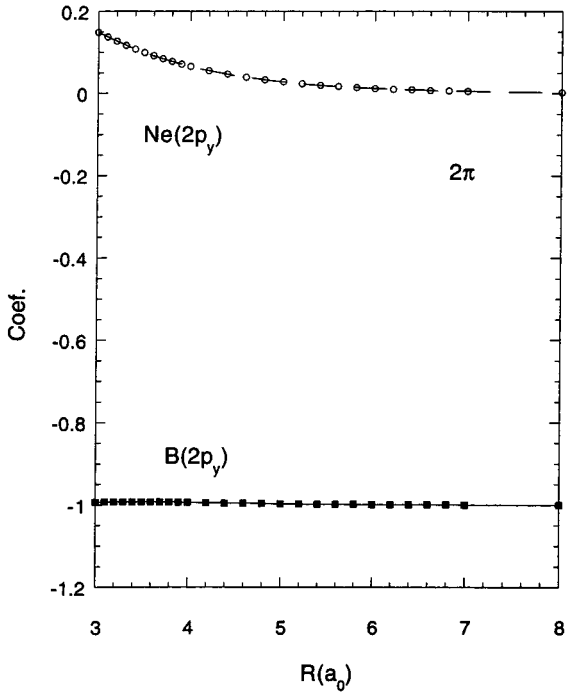

Figure 4. Dominant atom-centered basis function contributions to the $2\pi_y$ (nominally B $2p_y$) orbital. Squares denote the B $2p_y$ orbital. Open circles denote the Ne $2p_y$ orbital. The interaction is antibonding. Adjacent points are joined with line segments.

antibonding with decreasing R. Using eq 3 in eq 2 and retaining only single-center terms in the spin−orbit operator results in

$$H^{so}(1^4\Pi,C^2\Delta)(R) \approx s_1(R)r_1(R)\langle \mathrm{B}(2p_z)\ |h_x^{so}|\mathrm{B}(2p_y)\rangle - s_2(R)r_2(R)\ \langle \mathrm{Ne}(2p_z)|h_x^{so}|\mathrm{Ne}(2p_y)\rangle \qquad (4)$$

Clearly at large R the boron contribution dominates, but with decreasing R both s_2 and r_2 grow in and the neon term

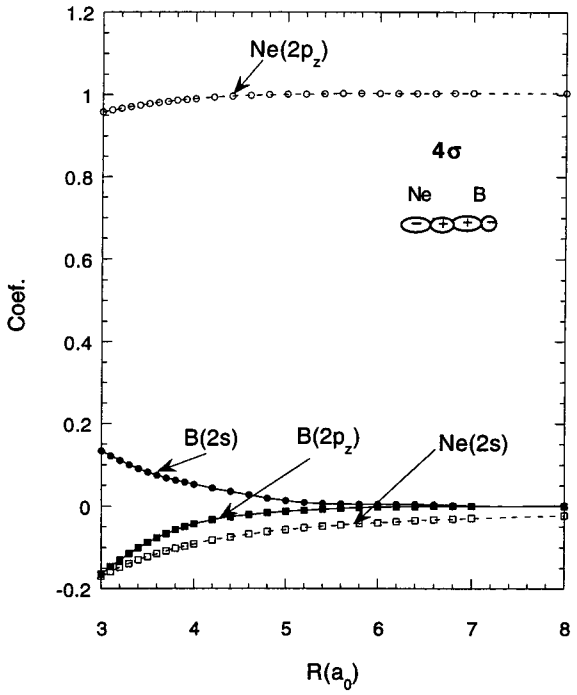

Figure 5. Dominant atom-centered basis function contributions to the 4σ (nominally Ne $2p_z$) orbital. Open circles denote the Ne $2p_z$ orbital. Solid circles denote the B 2s orbital, solid squares the B $2p_z$ orbital, and open squares the Ne 2s orbital. Adjacent points are joined with line segments.

contributes. This behavior is clearly evident in Figure 2. Since the neon cation spin−orbit coupling constant ($\zeta_{Ne} = -521$ cm^{-1})[26] has a much greater magnitude than that of atomic boron ($\zeta_B = 10.16$ cm^{-1}),[25] one expects the integral over neon orbitals to be considerably larger than that over boron orbitals. Modest contributions from neon in terms of s_2 and r_2 can therefore lead to a significant change in $H^{so}(1^4\Pi,C^2\Delta)(R)$. This is the external heavy atom effect (HAE). In our previous work on the BAr molecule, we found the HAE to be very pronounced.[13] While the effect is weaker here, contributions from the neon integral in eq 4 are still large enough to reverse the sign of the spin−orbit coupling at small internuclear separations. Interestingly, the HAE then results in a reduction of the spin−orbit interaction in the vicinity of R_e ($C^2\Delta$), although it ultimately increases the size of the interaction for shorter R.

A similar analysis has been used successfully in the interpretation of the structure of the R dependence of the fine-structure splitting in $1^2\Pi$ LiAr and LiNe.[27]

3.3. $C^2\Delta$ Bonding. Taking together the above analysis of the spin−orbit coupling and the clues from the electronic structure calculations, we are in a position to fully address the nature of the bonding in BNe $C^2\Delta$. The single CSF interpretation of the spin−orbit coupling revealed that the 6σ orbital (a partially sp-hybridized B $2p_z$ in the molecular region, see Figure 3) takes on principally Ne $2p_z$ character in an antibonding manner. The complementary bonding 4σ orbital is a partially sp-hybridized Ne $2p_z$ orbital but develops principally B $2p_z$ character in a bonding manner with decreasing R. (See Figure 5.) This orbital is essentially doubly occupied. Since Ne $2p_z$ is essentially doubly occupied in the atomic limit but B $2p_z$ is not, we see that a dative or coordinate covalent bond is being formed, just as in BAr.[13] The importance of this orbital can be seen in the CI calculations. The AS2−SOCI treatment, which does not correlate the 4σ orbital, greatly underestimates the bond strength of the $C^2\Delta$ state (see Figure 1). This effect is similar to that seen in isovalent BAr when the corresponding 6σ orbital is uncorrelated. The *degree* of dative bonding is much less than in BAr. The contribution of boron character to the 4σ orbital in BNe (as revealed by the coefficients on the boron-centered basis functions) is much smaller than the boron contribution to the corresponding 6σ orbital in BAr. In addition, the bond strength (D_e BAr $C^2\Delta \approx 3700$ cm^{-1}, D_e BNe $C^2\Delta \approx 138$ cm^{-1}) indicates that dative bonding is much less important in BNe. Nevertheless, the hybridization of the orbitals, the orbital populations, and the way D_e can be "switched on" by correlating the critical orbital, strongly support dative bonding as operative in BNe $C^2\Delta$.

TABLE 2: Predissociation Rates

ν	AS1−SOCI	AS1−SOCI/DC
0	1.1×10^{-5}	2.5×10^{-4}
1	3.3×10^{-5}	5.9×10^{-4}
2	1.1×10^{-5}	1.1×10^{-3}
3	1.1×10^{-3}	1.6×10^{-3}

[a] Calculated predissociation rates (in s^{-1}) for various vibrational levels ν of BNe $C^2\Delta$. Note that all rates effectively are zero.

3.4. Predissociation. Armed with reliable PECs and the associated spin−orbit coupling, we proceed to evaluate the magnitude of the spin−orbit induced predissociation of BNe $C^2\Delta$ by coupling to $1^4\Pi$. In the FGR approximation the predissociation rate is given by

$$A(C^2\Delta,\nu,J) = \frac{4\mu}{k}\langle\chi_{\nu,J}(C^2\Delta)|H^{so}(1^4\Pi,C^2\Delta)|\chi_{E,J}(1^4\Pi)\rangle \quad (5)$$

where $\chi_{\nu,J}(C^2\Delta)$ is an eigenfunction of the vibrational Schrödinger equation[28] in the Hund's case (a) limit and $\chi_{E,J}(1^4\Pi)$ is the continuum wave function for the repulsive $1^4\Pi$ state at the same energy. The predissociation rates for the vibrational levels of the $C^2\Delta$ state for $J = {}^3/_2$ and $\Omega = {}^3/_2$ are shown in Table 2. As previously inferred from spectroscopic studies,[12] the spin−orbit-induced predissociation is very close to nill and is of no consequence.

Experimental results indicate that the splitting of the rotational sublevels is very small indeed, on the order of a small fraction of a cm^{-1} and well below the precision of the present calculations.[12] In addition, the $C^2\Delta-1^4\Pi$ crossing is very high on the repulsive inner limb, which means that any nonnegligible contribution to the integral in eq 5 arises from the exponentially decaying tails of the vibrational wave functions, ergo there will be no dramatic fine-structure dependence of $A(C^2\Delta,\nu,J)$. In light of these facts, and the essentially zero predissociation rates, it is clear that a more complete treatment which includes the rotational sublevels in a Hund's case (b) description would be of no benefit. The present calculations unequivocally demonstrate that predissociation of BNe $C^2\Delta$ by $1^4\Pi$ is negligible.

4. Conclusions

Large-scale second-order configuration-interaction calculations involving more than 6.9 million CSFs have been performed on the $C^2\Delta$ and $1^4\Pi$ states of BNe. The spectroscopic parameters associated with the $C^2\Delta$ state are in very close accord with experimental results of refs 11 and 12.

Spin−orbit coupling of the $C^2\Delta$ and $1^4\Pi$ states has been computed based on the SOCI wave functions and used to compute the rate of predissociation for the vibrational levels of the $C^2\Delta$ state. The spin−orbit coupling exhibits the external heavy-atom effect, but to a lesser degree than in isovalent BAr. It is found that unlike BAr, in BNe, $1^4\Pi$ does not appreciably predissociate $C^2\Delta$. This is due principally to the location of the $C^2\Delta-1^4\Pi$ crossing which is found to occur very high on

the repulsive inner limb ($R_x = 3.17\ a_o$, approximately 4000 cm^{-1} above the $C^2\Delta$ dissociation asymptote), in accord with a previous experimental inference.[11,12]

Careful analysis of the $C^2\Delta-1^4\Pi$ spin−orbit coupling and the electronic structure reveals a degree of dative bonding in BNe $C^2\Delta$, but not to the extent seen in BAr, where it leads to an anomalously strong bond for a van der Waals system.

Acknowledgment. The present calculations were performed on IBM RS6000 workstations purchased with funds from AFOSR Grant AFOSR 90-0051, NSF Grant CHE 91-03299 and DOE BES Grant DE-FG02-91ER14189. The authors thank Prof. Paul Dagdigian and Xin Yang for numerous useful conversations concerning their experimental studies.

References and Notes

(1) Greenwood, N. N.; Earnshaw, A. *Chemistry of the Elements*; Pergamon Press: Oxford, 1984; Chapter 18.
(2) Purser, H. G.; *J. Chem.* Educ. **1988**, 65, 119.
(3) Breckenridge, W. H.; Jouvet, C.; Soep, B. In *Advances in Metal and Semiconductor Clusters*; Duncan, M., Ed.; JAI: Greenwich, 1995; Vol. III.
(4) Brazier, C. R.; Carrick, P. G. *J. Chem. Phys.* **1992**, 96, 8683.
(5) Manaa, M. R.; Yarkony, D. R. *J. Chem. Phys.* **1994**, 100, 8204.
(6) Massick, S.; Breckenridge, W. H. *J. Chem. Phys.* **1996**, 104, 7784.
(7) Massick, S.; Breckenridge, W. H. *J. Chem. Phys.* **1996**, 105, 6154.
(8) Yang, X.; Dagdigian, P. J. *J. Chem. Phys.* **1997**, 106, 6596.
(9) Amirav, A.; Evev, U.; Jortner, J. *Chem. Phys. Lett.* **1979**, 67, 9.
(10) Sohlberg, K.; Yarkony, D. R. *J. Chem. Phys.* **1997**, 106, 6607.
(11) Dagdigian, P. J.; Yang, X.; Hwang, E. In *Highly Excited States: Relaxation, Reactions, and Structure*; Edited by Mullin, A. J., Schatz, G. C., Eds.; ACS Symposium Series; American Chemical Society: Washington, DC. In press.
(12) Yang, X.; Hwang, E.; Dagdigian, P. J. *J. Chem. Phys.* **1996**, 104, 599.
(13) Sohlberg, K.; Yarkony, D. R. *J. Phys. Chem*., **1997**, 101, 3166.
(14) Docken, K.; Hinze, J. *J. Chem. Phys.* **1972**, 57, 4928.
(15) Hinze, J. *J. Chem. Phys.* **1973**, 59, 6424.
(16) Dunning, T. H., Jr. *J. Chem. Phys.* **1989**, 90, 1007.
(17) Langhoff, S. R.; Davidson, E. R. *Int. J. Quantum Chem.* **1974**, 8, 61.
(18) Prime, S.; Rees, C.; Robb, M. A. *Mol. Phys.* **1981**, 44, 173.
(19) Blomberg, M. R. A.; Siegbahn, P. E. M. *J. Chem. Phys.* **1983**, 78, 5682.
(20) Yarkony, D. R.; *Int. Rev. Phys. Chem.* **1992**, 11, 195.
(21) Rice, O. K.; *Phys. Rev.* **1929**, 33, 748.
(22) Rice, O. K.; *Phys. Rev.* **1929**, 34, 1451.
(23) Han, S.; Yarkony, D. R. *J. Chem. Phys.* **1995**, 103, 7336.
(24) Han, S.; Yarkony, D. R. *Mol. Phys.* **1996**, 88, 53.
(25) Odintzova, G. A.; Striganov, A. R. *J. Phys. Chem. Ref. Data*, **1979**, 8, 63.
(26) Moore, C. E. *Natl. Stand. Ref. Data Ser. (U.S., Natl. Bur. Stand.) 35/I*, (81), 1971.
(27) Sohlberg, K.; Yarkony, D. R. *J. Chem. Phys.* 1997. In press.
(28) Lefebvre-Brion, H.; Field, R. W. *Perturbations in the Spectra of Diatomic Molecules*; Academic Press: New York, 1986.
(29) Morse, P. M. *Phys. Rev.* **1929**, 34, 57.